Dynamic Nature of Host-Pathogen Interactions in *Mycobacterium marinum* Granulomas

DONNA M. BOULEY,[1] NAFISA GHORI,[2,3] K. LYNNE MERCER,[4]† STANLEY FALKOW,[2]
AND LALITA RAMAKRISHNAN[2]*

*Department of Comparative Medicine,[1] Department of Microbiology and Immunology,[2] and the Center for
Electron Microscopy,[3] Stanford University School of Medicine, Stanford, California 94305,
and 5371 Castleford Court, Newark, California 94560[4]*

***Mycobacterium marinum* causes long-term subclinical granulomatous infection in immunocompetent leopard frogs (*Rana pipiens*). These granulomas, organized collections of activated macrophages, share many morphological features with persistent human tuberculous infection. We examined organs of frogs with chronic *M. marinum* infection using transmission electron microscopy in conjunction with immunohistochemistry and acid phosphatase cytochemistry to better define the bacterium-host interplay during persistent infection. Bacteria were always found within macrophage phagosomes. These phagosomes were often fused to lysosomes, in sharp contrast to those formed during in vitro infection of J774 macrophage-like cells by *M. marinum*. The infected macrophages in frog granulomas showed various levels of activation, as evidenced by morphological changes, including epithelioid transformation, recent phagocytic events, phagolysosomal fusion, and disintegration of bacteria. Our results demonstrate that even long-term granulomas are dynamic environments with regard to the level of host cell activation and bacterial turnover and suggest a continuum between constantly replicating bacteria and phagocytic killing that maintains relatively constant bacterial numbers despite an established immune response. Infection with a mutant bacterial strain with a reduced capacity for intracellular replication shifted the balance, leading to a greatly reduced bacterial burden and inflammatory foci that differed from typical granulomas.**

Mycobacterium tuberculosis, the agent of human tuberculosis, most often causes a long-term asymptomatic infection called latent tuberculosis (19, 30, 31). Latently infected individuals have an approximately 10% lifetime risk of progressing to a highly contagious disease state called reactivation tuberculosis (19, 30, 31). This risk increases tremendously in immunocompromised individuals, such as those infected with human immunodeficiency virus (11, 12).

The latent stage of tuberculosis is characterized by granulomas (1). Granulomas are organized collections of mature macrophages that exhibit a certain typical morphology and arise in response to either a persistent intracellular pathogen or a foreign body (1). Mature granulomas evolve from an infiltrate of young mononuclear phagocytes that mature into macrophages, become activated, and aggregate. Activation is characterized by an increase in size and cytoplasmic organelles and a ruffled cell membrane, features which reflect their heightened phagocytic and microbicidal capacity (2, 14, 17, 19). In epithelioid granulomas, such as those caused by tuberculosis, the macrophages evolve further and differentiate into large epithelioid cells, which have tightly interdigitated cell membranes in zipper-like arrays linking adjacent cells as a cellular barrier to the extension of the infecting microorganisms. It is this host cell activation and organization of the infiltrate that distinguish the granuloma from simple chronic inflammation (1). Granulomas containing lymphocytes, extracellular matrix, calcification, and caseous necrosis are termed complex granulomas (1). The granuloma is thought to function to eradicate or contain inflammatory agents such as *M. tuberculosis* (52). The highly activated macrophages can kill many pathogens, and features such as the tight interdigitation of cell membranes and extracellular matrix may help to contain their spread. Yet the pathogenic mycobacteria are able to survive in the midst of this complex host response.

The granulomas harbor *M. tuberculosis*, and in humans and rabbits, but not in mice, they may have a central area of cellular debris called caseation (19, 48). Various studies have tried to determine the viability and virulence of *M. tuberculosis* in such lesions by attempting to culture the bacteria in axenic media and examining the virulence of tissue homogenates in experimental animals (21, 27, 32, 39, 51). These studies show that many asymptomatic humans harbor virulent bacteria in their tuberculous granulomas (39, 51). However, the metabolic and replicative state of the organisms in the granulomatous lesions of such asymptomatic humans remains a controversial subject. The bacteria could be in a metabolically and replicatively active state yet maintained in low numbers because the organism's rate of death (facilitated by host killing) is in equilibrium with its rate of replication. Alternatively, the bacteria could be in a nonreplicating state. Findings from different human studies as well as studies using animal models of tuberculosis can be interpreted to support both hypotheses (30, 31, 43). Determining the state of the bacteria during the so-called latent phase of infection would facilitate our understanding of the biology of latent tuberculosis. Latent tuberculosis represents a

* Corresponding author. Present address: Departments of Microbiology and Medicine, University of Washington, Box 357242, Health Sciences Building, 1959 NE Pacific St., Seattle, WA 98195-7242. Phone: (206) 616-4286. Fax: (206) 616-1575. E-mail: lalitar@u.washington.edu.
† Retired from the Department of Structural Biology, Stanford University School of Medicine, Stanford, CA 94305.

critical global public health problem, as one-third of the world's population is latently infected (29).

The relatively rapidly growing human and animal pathogen *Mycobacterium marinum* is used to understand the molecular pathogenesis of the chronic mycobacterioses, including tuberculosis (10, 40, 45, 46, 57). *M. marinum* produces a long-term asymptomatic infection in one of its natural hosts, the leopard frog (*Rana pipiens*). The infection is characterized by systemic granulomas that harbor relatively few organisms (46). The number of organisms within granulomas does not appear to change in the course of more than a year. The bacteria retain their virulence, since acute, fulminant disease results if the infected frogs are immunocompromised by the administration of corticosteroids. Rarely (approximately 1% of cases), even in the absence of corticosteroid treatment, frogs develop lethal *M. marinum* disease after more than a year of asymptomatic infection (R. H. Valdivia and L. Ramakrishnan, unpublished data).

M. marinum also replicates in cultured macrophages in a subcellular compartment indistinguishable from that occupied by *M. tuberculosis* (10, 44). In a screen for granuloma-induced *M. marinum* genes, we identified two types of activated genes: those expressed both in vitro in cultured macrophages and in vivo in granulomas, and those expressed exclusively in granulomas (45). These data suggested that the granuloma constitutes a complex environment with additional physiologic signals not produced by cultured macrophages. Our screen also revealed a variety of genes encoding metabolic and synthetic functions that are expressed in granulomas as well as in laboratory culture media (K. Chan, T. Knaak, L. Satkamp, S. Falkow, and L. Ramakrishnan, unpublished data). This suggests that the bacteria are in a transcriptionally active state in granulomas.

Results of gene expression studies led us to perform ultrastructural analyses to examine the nature of the granulomas in frogs chronically infected with *M. marinum*. The results of transmission electron microscopy (TEM) coupled with immunohistochemistry have shed light on the location of the bacteria within granulomas, the inflammatory cell response, and the dynamic nature of the host-pathogen interaction.

MATERIALS AND METHODS

Bacteria and macrophage cultures. The wild-type *M. marinum* strain M (44) and its isogenic mutant L1D, which has a disruption in the *mag* 24-1 gene (45), were grown as described previously (44, 45). The J774 A.1 (ATCC TIB67) mouse macrophage cell line was maintained as described previously (44).

Frogs. Young adult leopard frogs (*R. pipiens*), 5 to 6 cm long and purchased from J. M. Hazen (Alburg, Vt.), were maintained in accordance with the animal husbandry guidelines of Stanford University. They were inoculated with *M. marinum* so as to produce long-term asymptomatic granulomatous infection and examined as described previously (46). Livers and spleens of three frogs per time point were used for assessment of tissue histology and acid-fast staining by light microcy. Livers and spleens of six frogs were used for TEM studies: two at 17 weeks, two at 10 months, and two at 1 year postinfection. Immunoelectron microscopy was performed on samples from two frogs at 10 months postinfection, and acid phosphatase cytochemistry was performed on samples from one frog at 17 weeks postinfection. Tissue samples from each frog were plated for viable bacterial counts to ensure that they had maintained a chronic infection (46). The Internal Review Board of Stanford University approved all experimental procedures used with the frogs.

Persistence assays in J774 cells. A 7-day persistence assay using strain M was performed as described previously (46).

Microscopy. For histological examination, liver and spleen tissues were fixed in 10% buffered neutral formalin and processed for paraffin embedding. Sections (5 μm) were stained with hematoxylin and eosin (H&E) or acid-fast stains by Histo-Tec Laboratory (Hayward, Calif.). TEM of the J774 macrophage cell line was performed as described previously (44). Fresh tissues for TEM were processed in the same manner as the J774 cells except that they were fixed overnight in 2% glutaraldehyde fixative. Several hundred fields were examined. In the case of *M. marinum* L1D-infected frog liver, paraffin-embedded tissue was prepared for TEM as follows. The area of interest from the histologic slide was selected, and the corresponding area was excised from the block and cut into 1-mm-thick pieces. The tissues were immersed twice in xylene for 2 h each and then rehydrated by immersion through a series of graded ethanol concentrations for 30 min each. Tissues were placed in three changes of 0.1 M cacodylate buffer for 10 min each, fixed with 1% osmium tetroxide, and processed as described for TEM of fresh tissue.

Cells were identified and classified by their morphological resemblance to photographs of electron micrographs and descriptions of cells in various mammalian species (16, 33, 37, 38, 42, 49). Immunohistochemistry with a rabbit polyclonal serum to *M. marinum* (45) (gift of D. Brooks and P. L. C. Small) was performed as described previously (50). Briefly, the tissues were fixed at 4°C in 2% formaldehyde and 0.5% glutaraldehyde. They were stained using 1% uranyl acetate and dehydrated in ethanol as described for TEM. They were infiltrated at 4°C in steps using a graded combination of ethanol and LR white resin (Polysciences Incorporated, Warrington, Pa.) and embedded and polymerized in the LR white resin. The sections were incubated in a 1:500 dilution of the antibody and then in a 1:10 dilution of goat anti-rabbit immunoglobulin G serum conjugated to 10-nM gold particles (BB International, Burlingame, Calif.) and stained in 1% uranyl acetate and lead citrate prior to examination.

Acid phosphatase cytochemistry was performed as described previously (20, 22). Briefly, fresh tissue was cut into 2-mm-thick and 10-mm-wide sections, which were agitated at 4°C in 2% paraformaldehyde and 2.5% glutaraldehyde for 3 h. After rinsing in cacodylate buffer overnight at 4°C, 10- to 30-μm sections were cut into ice-cold 7.5% sucrose solution and transferred to a solution of 0.1% CMP and 0.12% lead acetate in 0.02 M sodium acetate buffer (pH 5.0). They were agitated in this solution for 20 to 40 min at 37°C, transferred back to 7.5% sucrose, fixed in osmium, and embedded as described above for TEM.

RESULTS

Light microscopy of *M. marinum*-infected tissues reveals variations in the morphology of granulomas. Histologic sections of infected frog livers stained with either H&E or acid-fast stains were examined. To assess the early stages of the immune response to *M. marinum*, we examined frog tissues 2 weeks postinfection. The most prominent host response was that of macrophage aggregates that lacked organization (Fig. 1e), rather than the tightly packed epithelioid granulomas seen in later stages (Fig. 1b). Rare mitotic figures were seen in macrophages in this early stage (Fig. 1e), suggesting some in situ cell division. Occasional bacteria were observed in these lesions (data not shown).

Granulomas were seen by 8 weeks postinfection and were comprised mostly of tightly packed cells which upon light microscopy displayed the typical indistinct cytoplasmic borders and abundant eosinophilic cytoplasm of epithelioid macrophages (1). Like the 2-week lesions, these granulomas also had sparse acid-fast bacilli (44, 46) (Fig. 1c). Occasional granulomas were comprised of a central area of epithelioid macrophages surrounded by small round cells with scant cytoplasm and hyperchromatic nuclei, consistent in appearance with lymphocytes (Fig. 1d).

***M. marinum* organisms are found within phagosomes of macrophages in mature granulomas.** We used TEM in conjunction with immunohistochemistry to determine the location of *M. marinum* in infected tissues (see Materials and Methods). Initially, livers from frogs chronically infected with *M.*
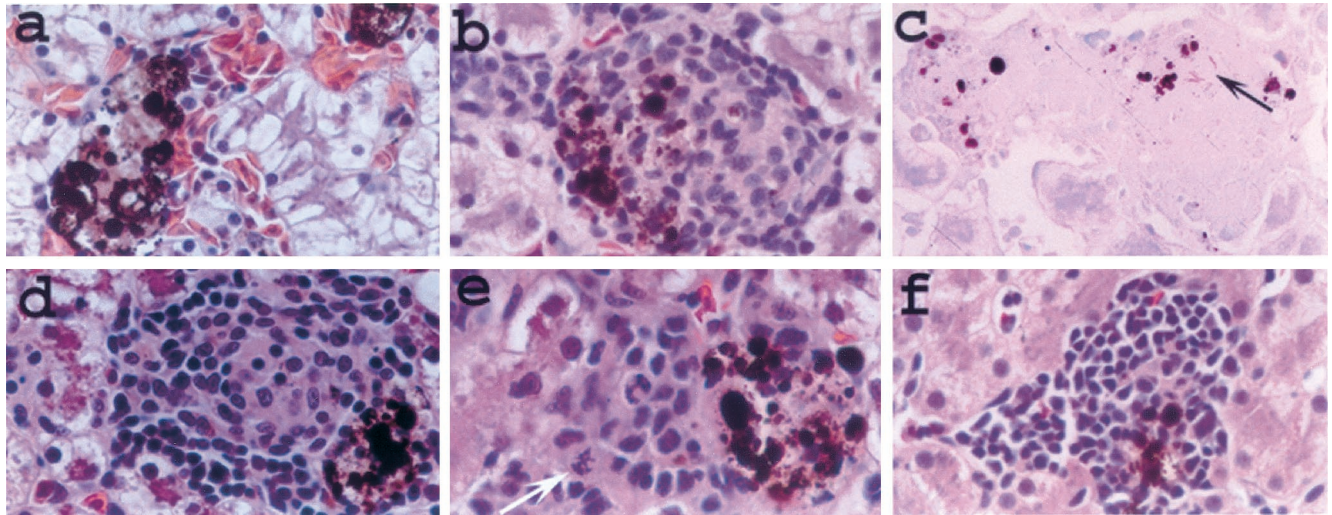
FIG. 1. Lesions produced in *M. marinum*-infected frogs. Sections from livers 8 weeks (a to d and f) and 2 weeks (e) postinfection were examined by light microscopy. (a) Uninfected liver section showing normal melanophage aggregates. Such aggregates of brown-black pigment-laden cells were distributed throughout the livers of uninfected frogs and associated with the granulomas of infected frogs (b and d to f). Such aggregates of pigmented cells are normal in the livers of *R. pipiens* and other species of frogs and are composed of melanin-containing macrophages (melanophages) (7). (b to e) Livers infected with wild-type *M. marinum*. (b and c) Typical granulomas during infection with *M. marinum* (arrow). (d) Less typical but not rare granuloma variation in wild-type infected livers. Note the mitotic figure in panel e (white arrow), suggestive of cell proliferation. (f) Typical mononuclear cell aggregate found in frogs infected with mutant strain L1D. All sections were stained with H&E except that in panel c, which was stained with an acid-fast (modified Ziehl-Neelsen) stain. Magnification, ×400.

marinum were scanned at low magnification by TEM to search for structures previously identified as bacteria (44). In order to verify that the structures we identified were in fact *M. marinum*, we used an immunogold TEM technique with rabbit polyclonal antisera to *M. marinum* to label tissues from chron-ically infected frogs (see Materials and Methods). The gold beads were localized only to those structures we had identified as *M. marinum* by TEM (Fig. 2).

Bacteria were most consistently found within granulomas. Of several hundred bacteria identified by scanning liver sec-
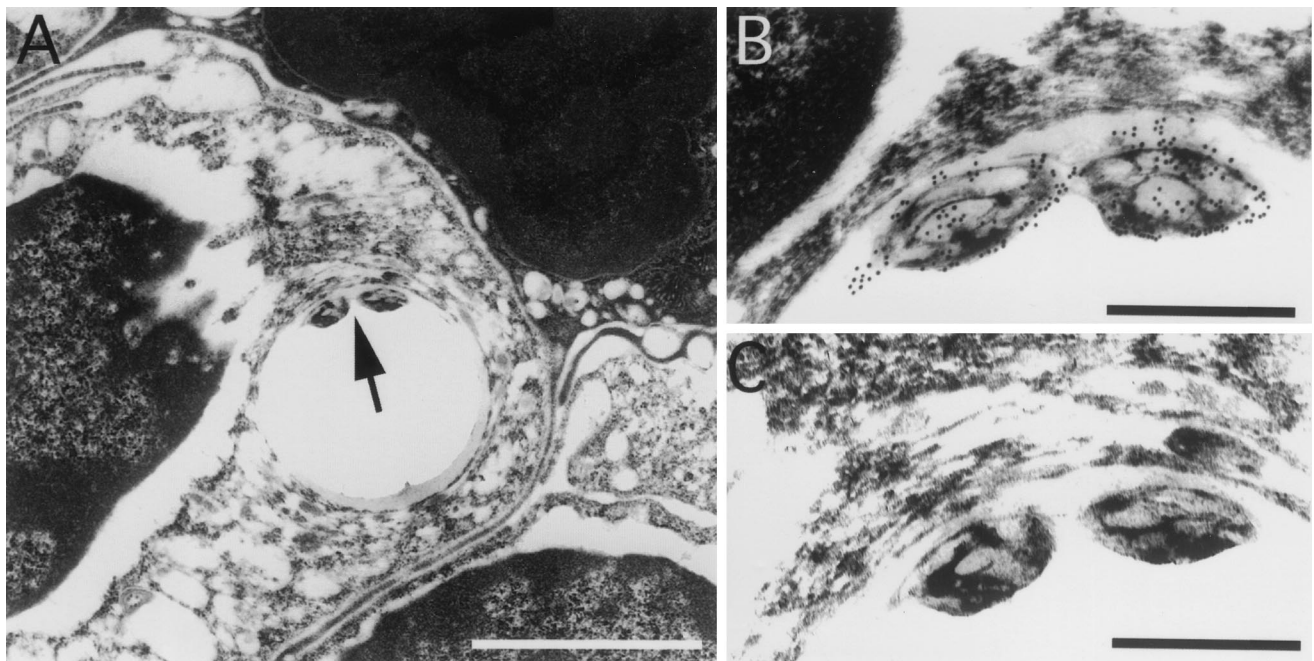

FIG. 2. *M. marinum* is located intracellularly within phagosomes in granulomas. (A) Immunohistochemistry of a 10-month spleen granuloma demonstrates bacteria within a phagosome (arrow). (B) Higher magnification of the *M. marinum* organisms in panel A showing specific labeling of the bacteria with antibody-conjugated gold particles. (C) Serial section stained without the primary antibody. No particles are seen. The phagosomes were often distorted due to artifactual tearing while exposed to the high beam of the electron microscope. The tearing was specific to regions that contained the bacteria and occurred over a range of infiltration and fixation procedures tested. Bars, 5 μm (A) and 0.5 μm (B and C).

tions at random, we saw only two outside a granuloma. Both of these were within a single hepatocyte (data not shown). The restriction of bacteria to granulomas was consistent with our observations by light microscopy, where acid-fast bacteria were detected only in granulomas.

Thus, bacteria in granulomas were always within macrophages (Fig. 2A and 3B and C) in membrane-bound cytoplasmic vacuoles (phagosomes) (Fig. 3B) rather than free in the cytoplasm or extracellular spaces.

Bacterial phagosomes are often fused to lysosomes. As reported previously, in J774 or RAW macrophages (10, 44), the bacterial phagosomes were neither fused to nor associated with lysosomes, even late in infection (Fig. 3A). However, within the granulomas of infected frogs, the bacteria were often in phagosomes closely associated with lysosomes, giving the appearance of fused compartments (phagolysosomes). Of the 70 bacteria examined in random fields, 41 were associated with phagolysosomes.

We utilized an enzymatic reaction which permits identification of the lysosomal enzyme acid phosphatase by converting it into granular deposits (20, 22). Following the acid phosphatase reaction, we confirmed the localization of bacteria to be often within fused phagolysosomes. Of interest is our finding that even within the same infected cell, some phagosomes were fused to lysosomes while others were not (Fig. 4). Figure 4A and B demonstrate phagosomes not fused to lysosomes. These phagosomes lack black deposits that represent acid phosphatase activity. In contrast, the bacteria in Fig. 4A, inset C, are fused to lysosomes. These three bacterial phagosomes all contained black deposits, confirming that fusion to lysosomes had occurred (Fig. 4C).

The activation state of infected macrophages varies within granulomas and correlates with the degree of phagolysosomal formation. Activated macrophages are associated with ultrastructural features, such as increased cytoplasmic organelles, including primary lysosomes, and the development of complex pseudopodia or ruffled cell membranes (1, 2). Primary lysosomes are present in moderately activated macrophages (14). In highly activated macrophages, the primary lysosomes fuse with phagocytic vacuoles to form secondary lysosomes, which become even more fusogenic and often engulf newly phagocytosed bacteria (14).

In contrast to infected, cultured J774 cells, which appeared to be quiescent and contained only rare lysosomes or organelles (Fig. 3), macrophages in granulomas exhibited features characteristic of higher activation states. For example, the macrophage shown in Fig. 3B was moderately activated and contained abundant mitochondria, Golgi, and primary lysosomes yet lacked secondary lysosomes and ruffled cell membranes (Fig. 3B and C). Consistently, nonfused bacterial phagosomes were found in macrophages exhibiting lower activation states (Fig. 3B), while bacteria in phagolysosomes and secondary lysosomes were found in the more highly activated macrophages (Fig. 3C).

Recent phagocytic events are still seen in highly activated macrophages of mature granulomas. The most numerous bacteria were seen in areas of chronic granulomas containing the most highly activated macrophages. Figure 5 demonstrates one such area. These macrophages are replete with secondary lysosomes and contain phagosomes surrounding viable bacteria
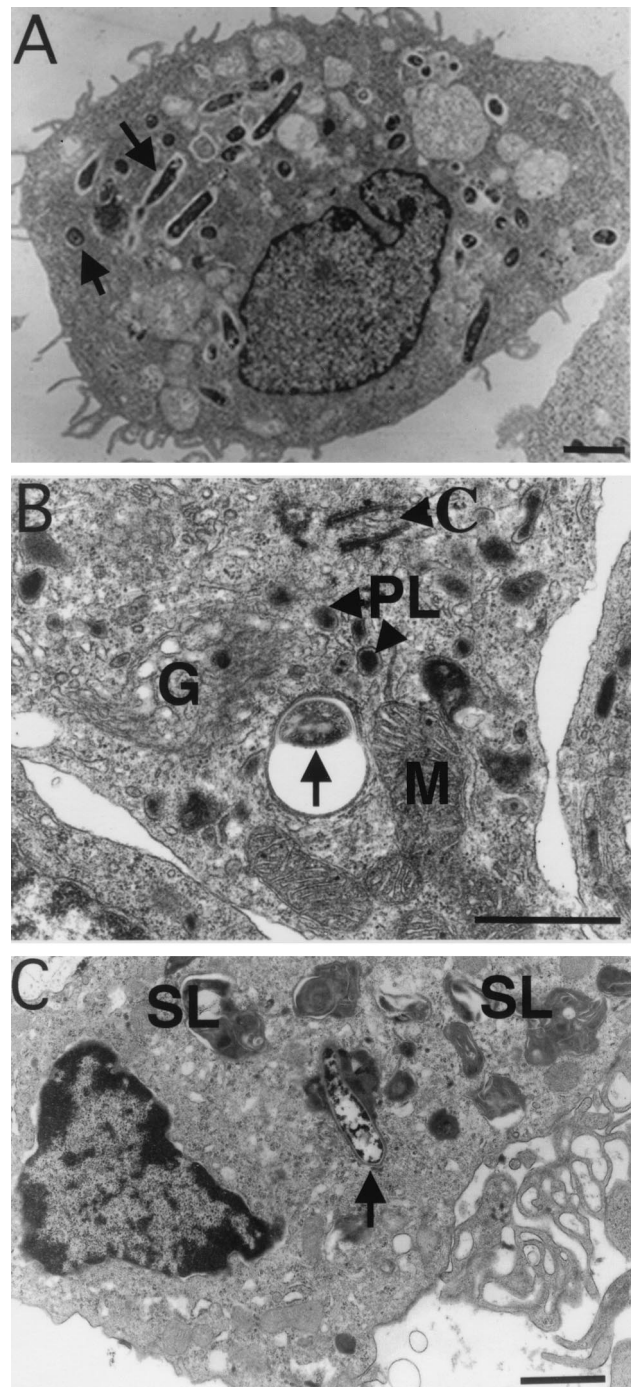

FIG. 3. *M. marinum* resides in either phagosomes or phagolysosomes in macrophages comprising granulomas. (A) TEM of *M. marinum* phagosomes (arrows) in J774 cells 7 days postinfection. The paucity of organelles is characteristic of quiescent or relatively inactive cells. (B and C) Macrophages in granulomas in spleens of frogs infected for 10 and 12 months, respectively. (B) Several organelles, indicative of cellular activation, are present in this macrophage, which contains a phagocytosed bacterium (arrow). (C) Cell exhibiting a high level of activation, including phagolysosomes (arrow), abundant secondary lysosomes, and prominent pseudopodia (ruffled edge). Bars, 2 μm (A and C) and 0.5 μm (B). SL, secondary lysosomes; PL, primary lysosomes; M, mitochondria; G, Golgi; C, centriole.
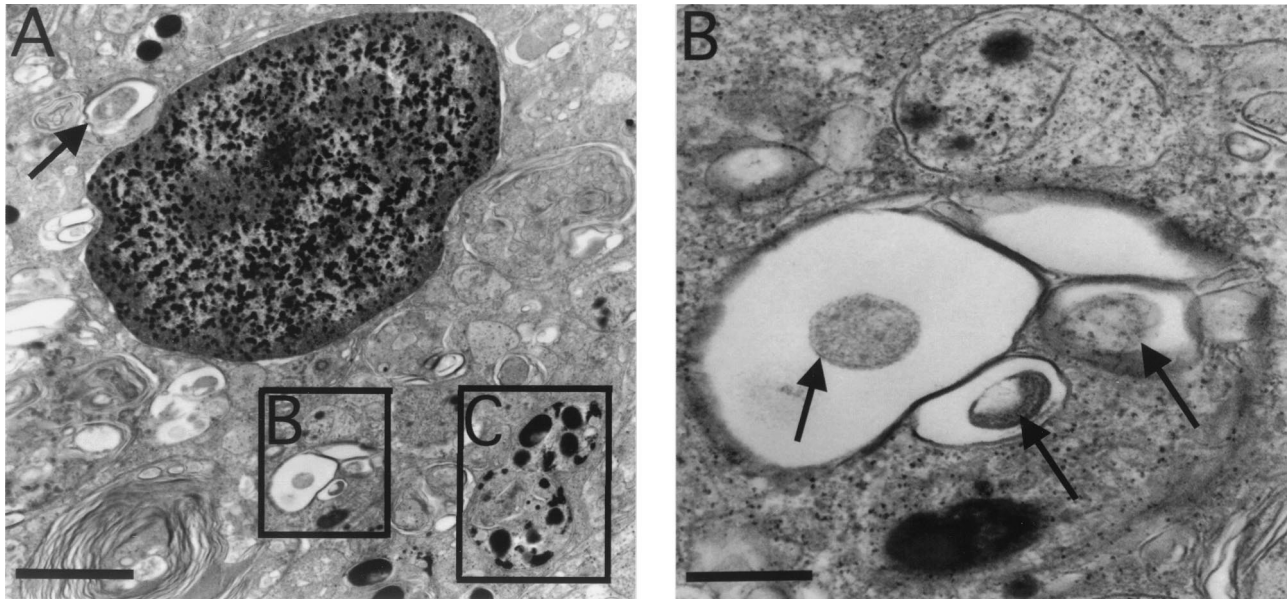
FIG. 4. Analysis of phagolysosomal fusion by acid phosphatase cytochemistry. (A) Macrophage in a granuloma from liver 17 weeks postinfection containing bacterial phagosomes not fused to lysosomes (arrow and inset B) and those fused to lysosomes, forming phagolysosomes (inset C). (B) Bacteria (arrows) in phagosomes lacking acid phosphatase activity characterized by black deposits. (C) Granules within phagosomes indicative of phagolysosomal fusion. Arrows, partially degraded bacteria in the phagolysosome. Bars, 2 μm (A) and 0.5 μm (B and C).

as well as bacteria in phagolysosomes. In close proximity to the plasma membrane of the macrophage is a large phagosome containing four bacteria which is surrounded by primary lysosomes, suggestive of impending fusion. Similarly, the phagosome in an adjacent macrophage also has primary lysosomes in close proximity.

Loosely interdigitated mature macrophages and epithelioid cells coexist in chronic *M. marinum* granulomas. Macrophages in tuberculous granulomas are thought to evolve during infection (1–3, 19). Loosely interdigitated mature macrophages are transformed over time into tightly interdigitated epithelioid cells (1–3). Reports in the literature identify two distinct types of epithelioid cells that differ with regard to their activation states and phagocytic capabilities (1, 14, 41, 42). Some studies suggest that epithelioid cells are primarily nonphagocytic, do not have secondary lysosomes, and may have a secretory function (41, 42). However, other investigators believe epithelioid cells to be the most highly phagocytic and microbicidal cells in granulomas (1, 14).

Our light-microscopic studies have shown that *M. marinum* granulomas evolve quickly from loose macrophage aggregates to tight clusters of epithelioid cells. Yet by TEM, chronically infected frog granulomas were found to be comprised of all three types of cells described above. Figure 6A shows highly activated, loosely interdigitated macrophages that contain bacteria. Figure 6B details the inset in Fig. 6A and shows the features of active phagocytosis and cellular activation: a phagosome in the process of fusing to primary lysosomes, secondary
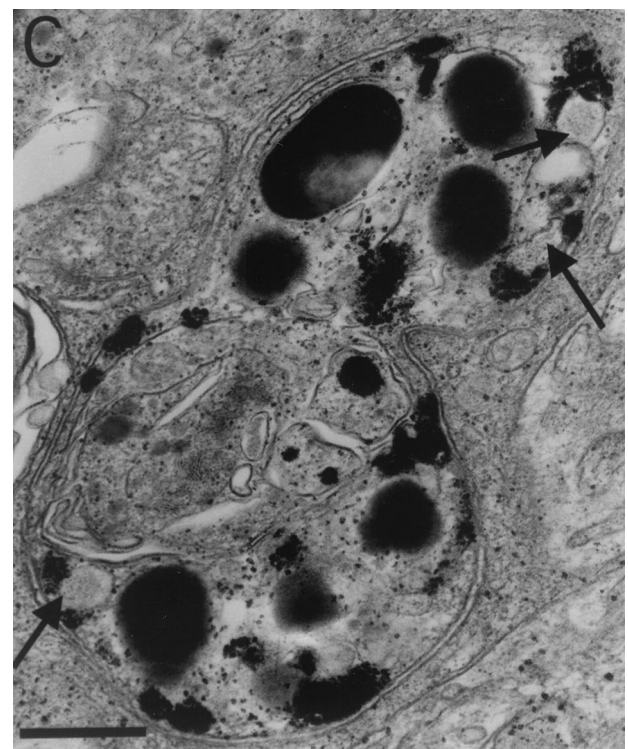
lysosomes, intermediate filaments, rough endoplasmic reticulum, and free ribosomes (1–3, 16).

Areas containing the two types of epithelioid cells characterized by tight interdigitations or zippering of pseudopodia are presented in Fig. 7. In Fig. 7A, the cells have tight cell membrane interdigitations, mitochondria, and primary lysosomes. However, they lack secondary lysosomes and contain only a few bacteria in nonfused phagosomes. Thus, these cells resemble the nonphagocytic (or secretory) epithelioid cells described previously (41, 42). The epithelioid cells in Fig. 7B also
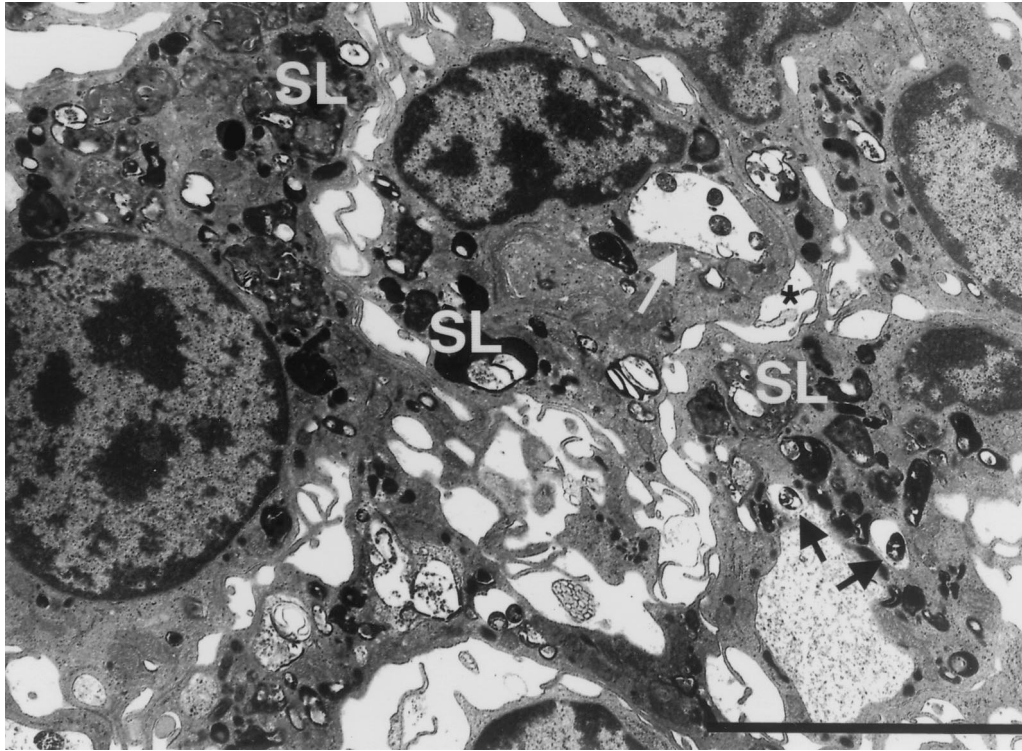
FIG. 5. Recent phagocytic events ongoing in highly activated macrophages of 17-week liver granulomas. White arrow, four bacteria in a phagosome close to the plasma membrane (asterisk) of the macrophage (considered recently formed). The phagosome has not yet undergone fusion to lysosomes, but primary lysosomes surrounding it suggest that fusion is imminent. Similarly, two bacteria (black arrows) in an adjacent macrophage are within nonfused phagosomes and are surrounded by primary lysosomes. The presence of numerous secondary lysosomes (SL), many fused to bacterial phagosomes, suggests a high level of activation in these resident macrophages found within this granuloma. Bar, 5 μm.

have tightly interdigitated pseudopodia yet contain multiple secondary lysosomes and numerous bacteria within fused and nonfused phagosomes, more typical of the phagocytic epithelioid cells described by most investigators (1, 14).

While most bacteria contained in phagolysosomes appeared to be intact, occasional degenerate bacteria were seen; Fig. 8 shows intact and degenerate bacteria within the same macrophage. The nonviable bacterium with a disintegrated membrane is contained within a large phagolysosome.

Epithelioid cells are a hallmark of the epithelioid and complex granulomas of mammalian *M. tuberculosis* infection (1). In addition to possessing the same continuum of macrophage-lineage cells, *M. marinum* granulomas exhibited additional features characteristic of mammalian tuberculous granulomas. The development of extracellular matrix proteins is a hallmark of mature granulomas (33), and this feature was noted in many *M. marinum* granulomas (Fig. 7B). Lymphocytes were also associated with granulomas, usually in close proximity to macrophages that appeared to be highly phagocytic and contained numerous secondary lysosomes (Fig. 6A and 8).

A mutant *M. marinum* produces infiltrates of macrophage precursors. L1D, a *M. marinum* strain with a mutation in *mag* 24-1, a gene of the PE-PGRS family that is expressed only in macrophages and granulomas, was described previously (45). This mutant does not persist in cultured macrophages and is attenuated in 8-week granulomas compared to wild-type bacteria. Our initial observations were that in two of four frogs, this mutant incited an atypical inflammatory infiltrate charac-

terized by loose aggregates of mononuclear cells (interpreted to be lymphocytes by light microscopy) (Fig. 1f), not seen in infections with wild-type bacteria (45). We extended these observations to include two more groups of three frogs each, infected with either the wild type or L1D for 8 weeks. We confirmed that 8-week infections in all of the L1D-infected frogs were characterized by collections of loose aggregates of mononuclear cells and only rare granulomas (Fig. 1f). Bacteria were not seen upon light microscopy with acid-fast stains in either type of lesion produced in the L1D-infected frogs (data not shown). This was consistent with the greatly reduced numbers of bacteria that were cultured from their organs at 8 weeks.

Examination of the loose cellular aggregates in the L1D-infected frogs by TEM identified these cells as early monocytes/immature macrophages rather than mature macrophages, typical of granulomas in frogs infected with wild-type bacteria (Fig. 9). Thus, the combination of light microscopy and TEM shows that these cellular aggregates are comprised predominantly of early monocytes/immature macrophages and lymphocytes. Consistent with the results from light microscopy, no bacteria were identified within these infiltrates by TEM (Fig. 9 and data not shown).

DISCUSSION

We performed a systematic microscopic examination of *M. marinum* granulomas ranging from 2 weeks to over 1 year
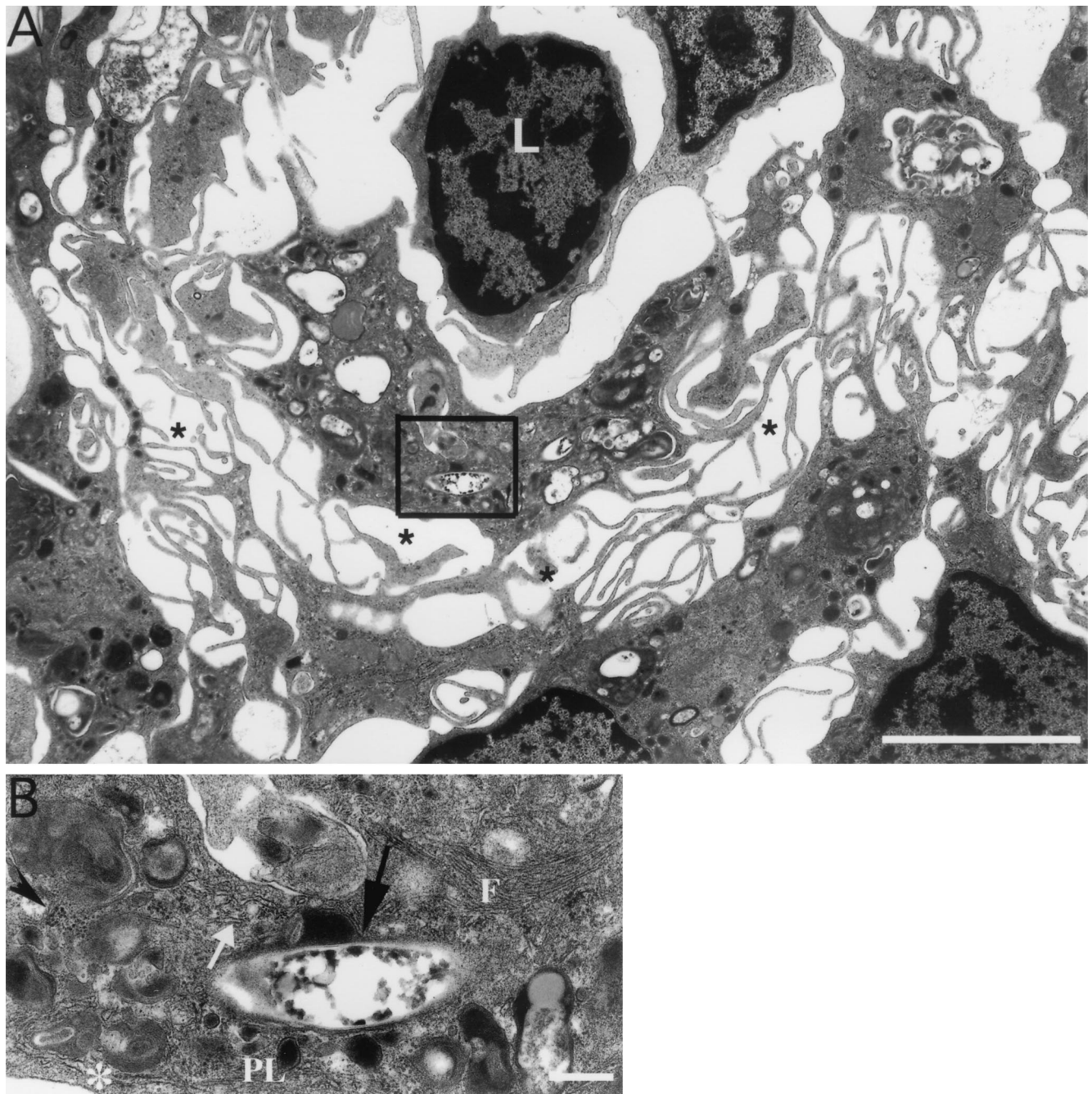
FIG. 6. Highly activated mature macrophages with loose intercellular interdigitations are present in mature granulomas. (A) One-year granulomas in liver in which the macrophages have loose interdigitations (asterisks), many phagocytosed bacteria, and secondary lysosomes. Lymphocytes (L) can occasionally be seen within granulomas of any duration. (B) Bacterial phagosome (black arrow) that is in the process of fusing with primary lysosomes (PL). Other markers of cellular activation, including secondary lysosomes, rough endoplasmic reticulum (asterisk), smooth endoplasmic reticulum (white arrow), free ribosomes (arrowhead), and intermediate filaments (F), are seen. Bars, 5 μm (A) and 0.5 μm (B).

postinfection. Surprisingly few ultrastructural studies of chronic mycobacterial lesions have been reported. Moreover, many conclusions about the ultrastructure of granulomas have been drawn from examination of tissues of laboratory animals infected with *Mycobacterium bovis* BCG or killed *M. tuberculosis* (2, 3, 38, 49). The granulomas produced in these studies were short-lived, as the inciting agents did not persist and the outcome of the host-pathogen interaction was essentially one

where the pathogen was cleared, a scenario that is quite different from infections with pathogenic mycobacteria. Only a few reports document the ultrastructure of lesions with virulent *M. tuberculosis* (33, 37). Similarly, the histochemical study of host-cell interactions in granulomas has also been performed using *M. bovis* BCG (4–6, 18, 54, 56). In this long-term ultrastructural study of a persistent mycobacterial infection, we have observed both similarities and differences with regard to
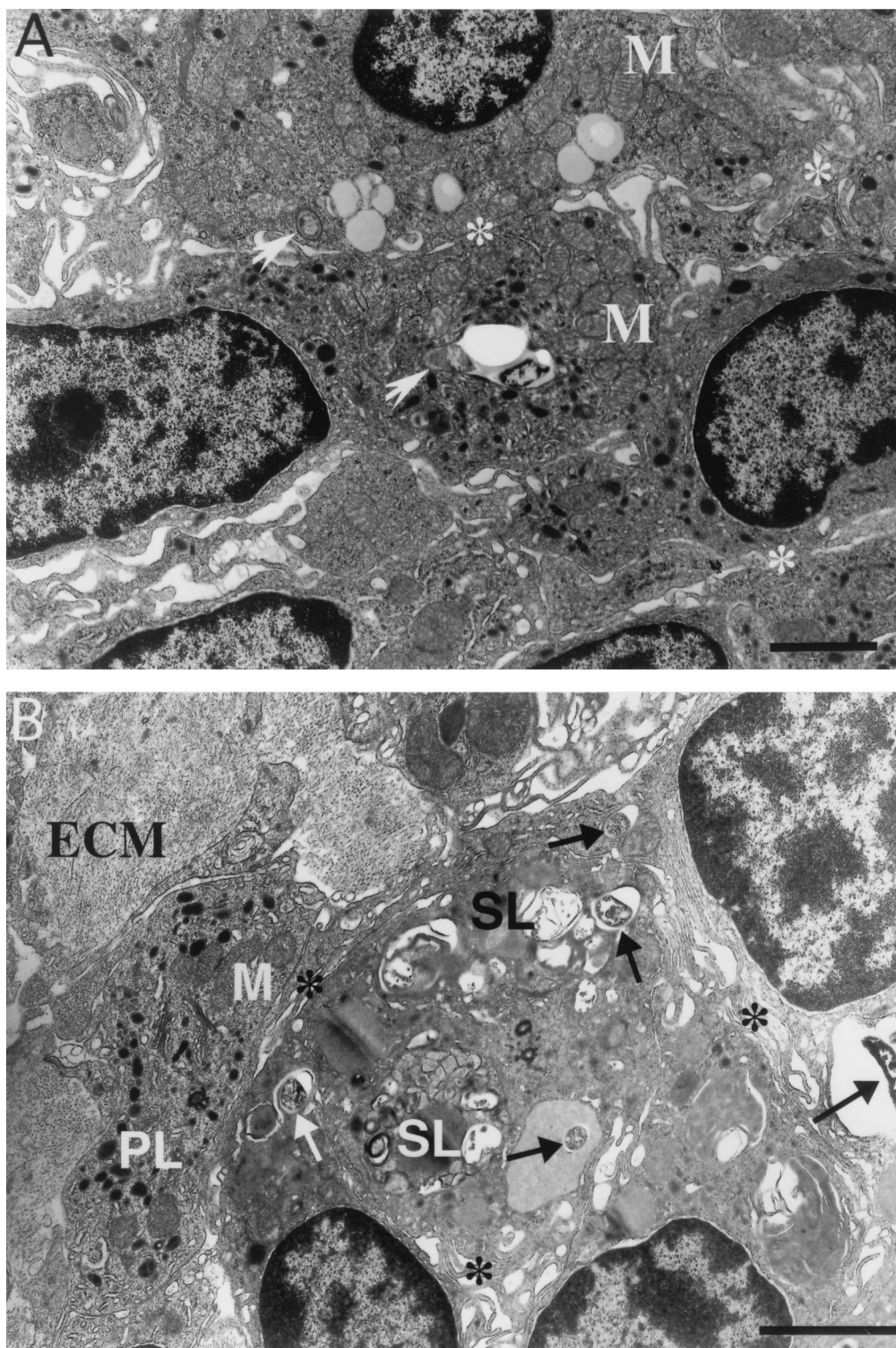
FIG. 7. Two types of epithelioid cell can be found in epithelioid granulomas. (A) Ten-month spleen granuloma made up of cells with closely apposed and tightly interdigitated pseudopodia (asterisks). These epithelioid cells are moderately active, contain primary but not secondary lysosomes, and demonstrate a relatively low level of phagocytosis. Two phagosomes (arrows) in the field are juxtaposed to primary lysosomes, indicating fusion initiation. (B) Ten-month liver granuloma also comprised of confluent cells with tightly interdigitated pseudopodia (asterisks) but containing numerous bacterial phagosomes (arrows) and secondary lysosomes (SL). Extracellular matrix (ECM) proteins, often associated with chronic granulomas, are present. PL, primary lysosomes; M, mitochondria; Bars, 5 μm.
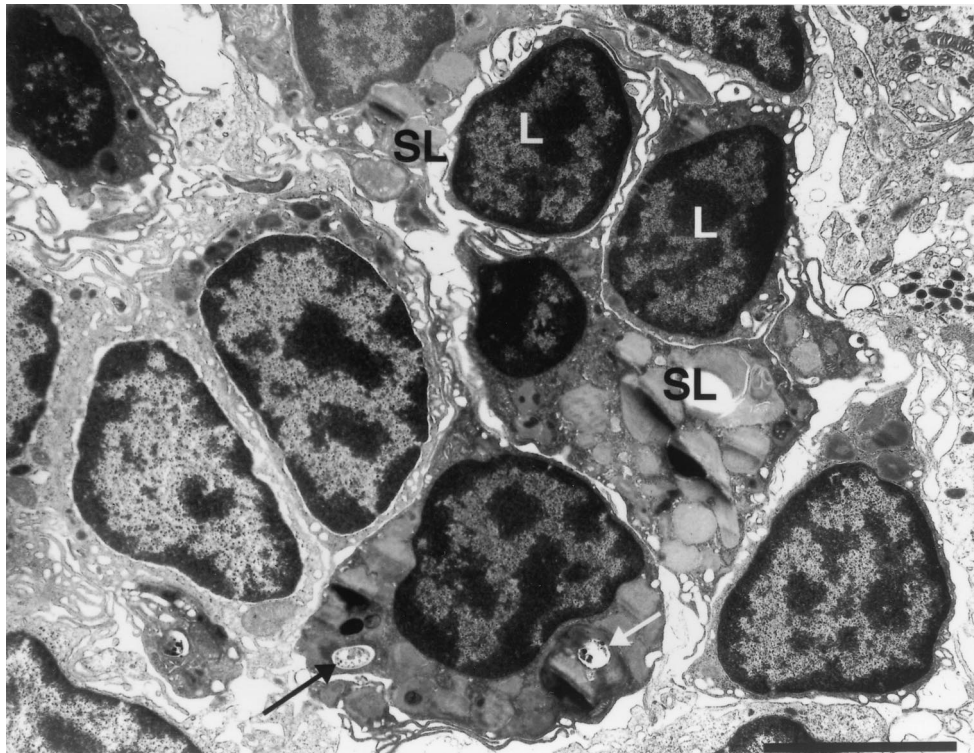
FIG. 8. Both viable and nonviable intracellular bacteria are found in granulomas. This 10-month liver granuloma is made up of a mixture of cell types, including lymphocytes (L), moderately activated macrophages, and highly activated macrophages containing numerous secondary lysosomes (SL). Black arrow, intact, presumably viable bacterium; white arrow, partially disintegrated bacterium in a large secondary lysosome. Bar, 5 μm.

the published literature. One important difference is that in *M. bovis* BCG granulomas, the more activated macrophages contain few intact bacteria or bacterial fragments (5, 42). In the chronic *M. marinum* granulomas, we see the reverse correlation: the more activated a cell appears to be, the more bacteria it contains. While this seems contradictory, it fits with the biology of the two infections. In both cases, the activated macrophages are likely the most phagocytic. However, in the case of *M. bovis* BCG, which does not persist, the bacteria are killed. In contrast, *M. marinum*, like *M. tuberculosis*, has the inherent capacity to counter macrophages and thus survives even in activated ones.

Light-microscopic (H&E) analysis has revealed that the lesions accompanying *M. marinum* infection of *R. pipiens* undergo a reproducible evolution of events. Within 2 weeks, infection incites loose macrophage aggregates, while tightly packed, epithelioid granulomas are consistently present by 8 weeks postinfection (46). After an initial increase, the number of organisms in infected tissue remains relatively constant over a very long period (46). However, the granulomas may increase in size over the course of the infection (46). We studied the ultrastructure of granulomas between 17 weeks and 1 year postinfection and found no qualitative differences in cell structure or organism localization between these time points. At the ultrastructural level, frog granulomas are virtually indistinguishable from those found in mammals (including humans) in terms of the morphology and spatial arrangement of the different cells (1–3, 16, 33, 38, 49).

The conventional view of tuberculous granulomas is one of

a central region of caseation, which contains bacilli in the stationary phase of growth. Surrounding this central region is a border of epithelioid macrophages and extracellular matrix components, which serve to wall off the offending organisms, as well as cytokine-secreting lymphocytes, which contribute to macrophage activation (1, 19, 23). Light microscopy of human tuberculous granulomas demonstrates organisms within macrophages as well as within the central caseous material. *M. marinum* granulomas in the frog share many features with human tuberculous ones, such as mature macrophages, epithelioid cells, and extracellular matrix components, yet lack caseation and giant cells. While *M. marinum* can cause caseous necrosis in humans, goldfish, and the toads *Xenopus laevis* and *Xenopus borealis* (9, 28, 57, 58), this does not appear to be a feature of *R. pipiens* granulomas. This is likely due to differences in the host response to infection—many frog species fail to undergo caseation, a phenomenon for which a pathological basis is not clear (7).

Despite the absence of obvious caseous necrosis, we thought it possible that the organisms contained within granulomas resided in an extracellular niche and that this might explain why some *M. marinum* genes are active only in granulomas and not in cultured macrophages (45). However, we failed to see extracellular bacteria despite exhaustive surveillance of infected tissues. These findings are in agreement with a previous TEM study of *M. tuberculosis* infection of mouse lung (37). While the location of bacteria is always intracellular, our findings offer a ready explanation for why the granuloma environment might convey different signals to the bacteria than those
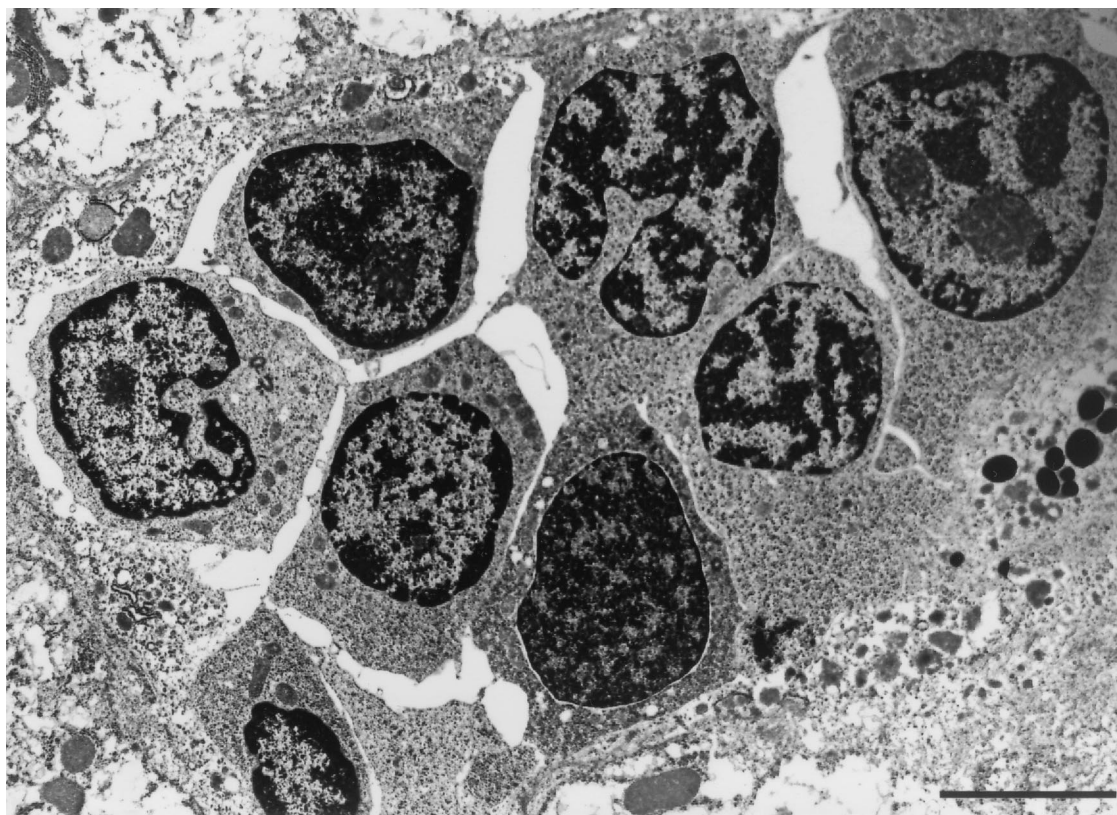
FIG. 9. Loose aggregates of monocytes/immature macrophages in an 8-week granuloma from a frog infected with the L1D mutant strain. Note the absence of ruffled cell membranes and interdigitations and a greater nuclear-to-cytoplasmic ratio in these cells compared to the activated macrophages in previous figures. Bar, 5 μm.

produced by cultured macrophages. The macrophages in granulomas were invariably more activated than in vitro macrophages. Their increased level of activation correlated with a high level of lysosomal fusion of the *M. marinum* phagosomes. Indeed, fully 60% of the *M. marinum* bacteria were within phagolysosomes. The other complexities unique to the granuloma apparent from this study, namely, the presence of epithelioid cells, lymphocytes, and extracellular matrix, may also alter the intracellular milieu of the bacteria and trigger distinct gene expression patterns.

The finding of *M. marinum* in phagolysosomes may seem surprising, since *M. marinum*, like *M. tuberculosis*, has been shown to avoid phagolysosomal fusion in macrophages in vitro (10, 13, 60). One general hypothesis has been that it is this "escape" from the phagolysosome that is the key to the bacteria's long-term survival. However, *Mycobacterium* phagosomes become fused to lysosomes if the bacteria are pretreated with the serum of *M. bovis* BCG-immunized rabbits (8). Furthermore, the intracellular survival and replication of *M. tuberculosis* were unaffected by the induction of phagolysosome fusion in this manner (8). Phagosome-lysosome fusion of *M. tuberculosis* is also induced upon infection of cytokine-activated macrophages (53, 59). In light of these studies, frequent observation of *M. marinum* in phagolysosomes within activated cells in vivo is hardly surprising. The intracellular pathogen *Legionella pneumophila*, which was also thought to resist phagosomal fusion, has been shown recently to reside in phagoly-

sosomes during long-term infection of macrophages (55). Similarly, the persistent pathogen *Cryptococcus neoformans* has also been shown to have a different location in vivo than in cultured cells (22).

Our study does not directly address the viability of the bacteria in phagolysosomes. The majority of bacteria in phagolysosomes appear to be morphologically intact and may be viable; occasional bacteria are clearly partially degraded and nonviable. However, it could be argued that nonviable mycobacteria remain intact for long periods owing to the complex lipid-rich nature of their cell walls (47). The finding that bacteria are in both fused and nonfused compartments within the same macrophage in a granuloma suggests several possibilities. Some of the in vivo-expressed genes may protect the bacteria from the ill effects of phagolysosomal fusion and other consequences of macrophage activation in granulomas. Two in vivo-induced *M. marinum* genes are activated by their acidic environment (K. Chan, T. Knaak, L. Satkamp, S. Falkow, and L. Ramakrishnan, unpublished data), supporting this hypothesis. Alternatively, phagolysosomal fusion could represent an inexorable pathway to death for every bacterium in the granuloma. A third possibility is that there are at least two populations of bacteria in the granulomas that occupy distinct intracellular niches and consequentially may have distinct intracellular fates. The few bacteria in the less activated macrophages that are in unfused phagosomes may represent those in a privileged niche destined for long-term survival. Such physiological het-

erogeneity in the populations of *M. tuberculosis* in human infections has been proposed (34). We did observe extremely rare bacteria in normal tissues outside the granulomas. These observations are consistent with those of others who have found evidence of *M. tuberculosis* infection in normal tissues of latently infected hosts (26, 39). However, their vanishingly small numbers make it extremely unlikely that these bacteria contributed to the gene expression profiles detected by our screen.

Since both the host cell response and the number of viable bacteria remain essentially the same in granulomas over the course of 1 year, we speculate that there is equilibrium between bacterial replication and death. Similarly, there appears to be a repeated spectrum of macrophage differentiation in granulomas over time. Thus, our studies demonstrate that even an epithelioid granuloma is an area of highly dynamic interactions between pathogen and host; the granuloma is far from a static entity. Our data suggest a model in which there may be an ongoing cycle of replication of bacteria within a particular class of immune cells and eventual bacterial destruction by activated cells with the morphological appearance of activated macrophages. We expect there is a parallel turnover of host cells and bacteria during this prolonged stage of the disease. Indeed, we see evidence of in situ macrophage division but infrequently and only in early infiltrates. Our finding of macrophages at different stages of maturation in chronic granulomas suggests that mononuclear cells are being recruited into the granuloma and are undergoing maturation there. This finding is consistent with previous observations (4). *Mycobacterium* granulomas are thought to have a high cell turnover, unlike those caused by inert foreign bodies (1, 6, 42). We presume this to be the case for *M. marinum* granulomas. However, we failed to see the occasional apoptotic bodies seen in *M. bovis* BCG granulomas (15).

It is noteworthy that we see in chronic granulomas both types of epithelioid cells reported in the literature (1, 14, 41, 42). It may be that macrophages can differentiate into at least two types of epithelioid cells: the cells with numerous secondary lysosomes carry out phagocytic events while the other type carries out secretory functions modulating the maintenance of the granulomas. Bacterial replication may occur predominantly in the phagocytic cells, while the secretory cells may contain the spread of infection. Alternatively, as proposed earlier, the secretory epithelioid cells may actually provide a safe haven for a few bacteria.

The mutant strain L1D gives rise predominantly to infiltrates consisting of loosely juxtaposed immature macrophages. Few bacteria are seen in such lesions, consistent with its decreased survival in both cultured macrophages and granulomas (45). This altered cellular response is not always associated with mutants attenuated in granulomas. Other mutants led to decreased numbers and size of granulomas but did not result in fundamental changes in granuloma morphology (46). An *M. tuberculosis* persistence mutant with a mutation in a protein involved in mycolic acid modification also altered the host immune response (24). In this case, pure lymphocytic aggregates were found. The findings with the *M. marinum* L1D mutant, which has a mutation in *mag* 24, suggest that specific proteins such as MAG 24 may potentiate macrophage differentiation either directly or indirectly. Since wild-type bacteria

survive better than the mutant in the granuloma, it could be argued that an essential strategy for latent infection is to deliberately induce macrophage differentiation into epithelioid cells. This may sound counterintuitive, but no more so than the finding that *Salmonella* and *Shigella* induce a proinflammatory response as a prerequisite to traveling from the Peyer's patches to mesenteric lymph nodes in order to spread systemically (35, 36, 61).

Our study has provided "snapshots" of the dynamic range of a persistent mycobacteriosis, a complex lifelong infection. It may shed light on a long-ranging controversy regarding whether the bacteria in chronic tuberculous lesions are in a truly latent (i.e., nonreplicating) state (25, 30, 31, 43). In a situation where there is no change in bacterial numbers and no progression to disease over 1 year, we find evidence of bacterial turnover and continuing infection of new host cells. Our results point to a functional rather than physiologic latency at least for some chronic mycobacterioses. Furthermore, our results reemphasize the importance of the direct examination of infected tissue rather than relying on in vitro systems (31). Additional studies comparing wild-type and mutant bacteria should yield more insight into how the bacteria manipulate the host cell response in order to dwell in this complex and seemingly adverse environment. The model system we employ may reflect some attributes of persistent (latent) tuberculosis in humans. Although the frog model has some limitations, we have found it useful in formulating hypotheses that may be tested in the more complex and experimentally more difficult study of *M. tuberculosis*.

REFERENCES

1. **Adams, D. O.** 1976. The granulomatous inflammatory response. A review. Am. J. Pathol. **84:**164–191.
2. **Adams, D. O.** 1974. The structure of mononuclear phagocytes differentiating in vivo. I. Sequential fine and histologic studies of the effect of Bacillus Calmette-Guerin (BCG). Am. J. Pathol. **76:**17–48.
3. **Adams, D. O.** 1975. The structure of mononuclear phagocytes differentiating in vivo. II. The effect of *Mycobacterium tuberculosis*. Am. J. Pathol. **80:**101–116.
4. **Ando, M., and A. M. Dannenberg, Jr.** 1972. Macrophage accumulation, division, maturation, and digestive and microbicidal capacities in tuberculous lesions. IV. Macrophage turnover, lysosomal enzymes, and division in healing lesions. Lab. Investig. **27:**466–472.
5. **Ando, M., A. M. Dannenberg, Jr., and K. Shima.** 1972. Macrophage accumulation, division, maturation and digestive and microbicidal capacities in tuberculous lesions. II. Rate at which mononuclear cells enter and divide in primary BCG lesions and those of reinfection. J. Immunol. **109:**8–19.
6. **Ando, M., A. M. Dannenberg, Jr., M. Sugimoto, and B. S. Tepper.** 1977. Histochemical studies relating the activation of macrophages to the intracellular destruction of tubercle bacilli. Am. J. Pathol. **86:**623–633.
7. **Anver, M. R., and C. L. Pond.** 1984. Biology and diseases of amphibians, p. 427–447. *In* J. G. Fox, B. J. Cohen, and F. M. Loew (ed.), Laboratory animal medicine. Academic Press, Orlando, Fla.
8. **Armstrong, J. A., and P. D. Hart.** 1975. Phagosome-lysosome interactions in cultured macrophages infected with virulent tubercle bacilli. Reversal of the usual nonfusion pattern and observations on bacterial survival. J. Exp. Med. **142:**1–16.
9. **Asfari, M.** 1988. Mycobacterium-induced infectious granuloma in Xenopus: histopathology and transmissibility. Cancer Res. **48:**958–963.
10. **Barker, L. P., K. M. George, S. Falkow, and P. L. Small.** 1997. Differential trafficking of live and dead *Mycobacterium marinum* organisms in macro-

phages. Infect. Immun. **65:**1497–1504.

11. **Barnes, P. F., A. B. Bloch, P. T. Davidson, and D. E. Snider, Jr.** 1991. Tuberculosis in patients with immunodeficiency virus infection. N. Engl. J. Med. **324:**1644–1650.

12. **Chaisson, R. E., and C. A. Benson.** 1995. Tuberculosis and HIV infection, p. 223–238. *In* M. D. Rossman, and R. R. MacGregor (ed.), Tuberculosis. McGraw-Hill, New York, N.Y.

13. **Clemens, D. L., and M. A. Horwitz.** 1995. Characterization of the *Mycobacterium tuberculosis* phagosome and evidence that phagosomal maturation is inhibited. J. Exp. Med. **181:**257–270.

14. **Cohn, Z. A.** 1968. The structure and function of monocytes and macrophages. Adv. Immunol. **9:**163–214.

15. **Cree, I. A., S. Nurbhai, G. Milne, and J. S. Beck.** 1987. Cell death in granulomata: the role of apoptosis. J. Clin. Pathol. **40:**1314–1319.

16. **Cross, P. C., and K. L. Mercer.** 1993. Cell and tissue ultrastructure. A functional perspective. W.H. Freeman and Company, Salt Lake City, Utah.

17. **Dannenberg, A. M., Jr.** 1968. Cellular hypersensitivity and cellular immunity in the pathogenesis of tuberculosis: specificity, systemic and local nature, and associated macrophage enzymes. Bacteriol. Rev. **32:**85–102.

18. **Dannenberg, A. M., Jr., M. Ando, and K. Shima.** 1972. Macrophage accumulation, division, maturation, and digestive and microbicidal capacities in tuberculous lesions. III. The turnover of macrophages and its relation to their activation and antimicrobial immunity in primary BCG lesions and those of reinfection. J. Immunol. **109:**1109–1121.

19. **Dannenberg, A. M., Jr.** 1993. Immunopathogenesis of pulmonary tuberculosis. Hosp. Pract. **28:**51–58.

20. **Doty, S. B., C. E. Smith, A. R. Hand, and C. Oliver.** 1977. Organic trimetaphosphatase as a histochemical marker for lysosomes in light and electron microscopy. J. Histochem. Cytochem. **25:**1381–1384.

21. **Feldman, W. H., and A. H. Baggenstoss.** 1939. The occurrence of virulent tubercle bacilli in presumably non-tuberculous lung tissue. Am. J. Pathol. **5:**501–515.

22. **Feldmesser, M., Y. Kress, P. Novikoff, and A. Casadevall.** 2000. *Cryptococcus neoformans* is a facultative intracellular pathogen in murine pulmonary infection. Infect. Immun. **68:**4225–4237.

23. **Flynn, J. L., and J. Chan.** 2001. Immunology of tuberculosis. Annu. Rev. Immunol. **19:**93–129.

24. **Glickman, M. S., J. S. Cox, and W. R. Jacobs, Jr.** 2000. A novel mycolic acid cyclopropane synthetase is required for coding, persistence, and virulence of *Mycobacterium tuberculosis*. Mol. Cell. **5:**717–727.

25. **Glickman, M. S., and W. R. Jacobs, Jr.** 2001. Microbial pathogenesis of Mycobacterium tuberculosis: dawn of a discipline. Cell **104:**477–485.

26. **Hernandez-Pando, R., M. Jeyanathan, G. Mengistu, D. Aguilar, H. Orozco, M. Harboe, G. A. Rook, and G. Bjune.** 2000. Persistence of DNA from *Mycobacterium tuberculosis* in superficially normal lung tissue during latent infection. Lancet **356:**2133–2138.

27. **Hobby, G. L., O. Auerbach, T. F. Lenert, M. J. Small, and J. V. Comer.** 1954. The late emergence of *M. tuberculosis* in liquid cultures of pulmonary lesions resected from humans. Am. Rev. Tuberc. **70:**191–218.

28. **Huminer, D., S. D. Pitlik, C. Block, L. Kaufman, S. Amit, and J. B. Rosenfeld.** 1986. Aquarium-borne *Mycobacterium marinum* skin infection. Report of a case and review of the literature. Arch. Dermatol. **122:**698–703.

29. **Maher, D., and M. C. Raviglione.** 1999. The global epidemic of tuberculosis: a World Health Organization perspective. *In* D. Schlossberg (ed.), Tuberculosis and nontuberculous mycobacterial infections. W.B. Saunders Company, Philadelphia, Pa.

30. **Manabe, Y. C., and W. R. Bishai.** 2000. Latent *Mycobacterium tuberculosis*—persistence, patience, and winning by waiting. Nat. Med. **6:**1327–1329.

31. **McKinney, J. D.** 2000. In vivo veritas: the search for TB drug targets goes live. Nat. Med. **6:**1330–1333.

32. **Medlar, E. M., S. Bernstein, and D. M. Stewart.** 1952. A bacteriologic study of resected tuberculous lesions. Am. Rev. Tuberc. **66:**36–43.

33. **Miller, R. L., D. J. Krutchkoff, and B. S. Giammara.** 1978. Human lingual tuberculosis. An ultrastructural study. Arch. Pathol. Lab. Med. **102:**360–365.

34. **Mitchison, D. A.** 1979. Basic mechanisms of chemotherapy. Chest **76:**771–781.

35. **Monack, D., and S. Falkow.** 2000. Apoptosis as a common bacterial virulence strategy. Int. J. Med. Microbiol. **290:**7–13.

36. **Monack, D. M., D. Hersh, N. Ghori, D. Bouley, A. Zychlinsky, and S. Falkow.** 2000. *Salmonella* exploits caspase-1 to colonize Peyer's patches in a murine typhoid model. J. Exp. Med. **192:**249–258.

37. **Moreira, A. L., J. Wang, L. Tsenova-Berkova, W. Hellmann, V. H. Freedman, and G. Kaplan.** 1997. Sequestration of *Mycobacterium tuberculosis* in tight vacuoles in vivo in lung macrophages of mice infected by the respiratory route. Infect. Immun. **65:**305–308.

38. **Narayanan, R. B., P. Badenoch-Jones, and J. L. Turk.** 1981. Experimental mycobacterial granulomas in guinea pig lymph nodes: ultrastructural observations. J. Pathol. **134:**253–265.

39. **Opie, E. L., and J. D. Aronson.** 1927. Tubercle bacilli in latent tuberculous lesions and in lung tissue without tuberculous lesions. Arch. Pathol. Lab. Med. **4:**1–21.

40. **Pagan-Ramos, E., J. Song, M. McFalone, M. H. Mudd, and V. Deretic.** 1998. Oxidative stress response and characterization of the *oxyR-ahpC* and *furA-katG* loci in *Mycobacterium marinum*. J. Bacteriol. **180:**4856–4864.

41. **Papadimitriou, J. M., and W. G. Spector.** 1971. The origin, properties and fate of epithelioid cells. J. Pathol. **105:**187–203.

42. **Papadimitriou, J. M., and W. G. Spector.** 1972. The ultrastructure of high- and low-turnover inflammatory granulomata. J. Pathol. **106:**37–43.

43. **Parrish, N. M., J. D. Dick, and W. R. Bishai.** 1998. Mechanisms of latency in Mycobacterium tuberculosis. Trends Microbiol. **6:**107–112.

44. **Ramakrishnan, L., and S. Falkow.** 1994. *Mycobacterium marinum* persists in cultured mammalian cells in a temperature-restricted fashion. Infect. Immun. **62:**3222–3229.

45. **Ramakrishnan, L., N. A. Federspiel, and S. Falkow.** 2000. Granuloma-specific expression of Mycobacterium virulence proteins from the glycine-rich PE-PGRS family. Science **288:**1436–1439.

46. **Ramakrishnan, L., R. H. Valdivia, J. H. McKerrow, and S. Falkow.** 1997. *Mycobacterium marinum* causes both long-term subclinical infection and acute disease in the leopard frog (*Rana pipiens*). Infect. Immun. **65:**767–773.

47. **Rees, R. J. W., and P. D. Hart.** 1961. Analysis of the host-parasite equilibrium in chronic murine tuberculosis by total and viable bacillary counts. Br. J. Exp. Pathol. **42:**83–88.

48. **Rhoades, E. R., A. A. Frank, and I. M. Orme.** 1997. Progression of chronic pulmonary tuberculosis in mice aerogenically infected with virulent Mycobacterium tuberculosis. Tuber. Lung Dis. **78:**57–66.

49. **Ridley, M. J., C. J. Heather, I. Brown, and D. A. Willoughby.** 1983. Experimental epithelioid cell granulomas, tubercle formation and immunological competence: an ultrastructural analysis. J. Pathol. **141:**97–112.

50. **Robards, A. W., and A. J. Wilson (ed.).** 1993. Procedures in electron microscopy. Wiley, New York, N.Y.

51. **Robertson, H. E.** 1933. The persistence of tuberculous infections. Am. J. Pathol. **9:**S711–S718.

52. **Saunders, B. M., A. A. Frank, and I. M. Orme.** 1999. Granuloma formation is required to contain bacillus growth and delay mortality in mice chronically infected with *Mycobacterium tuberculosis*. Immunology **98:**324–328.

53. **Schaible, U. E., S. Sturgill-Koszycki, P. H. Schlesinger, and D. G. Russell.** 1998. Cytokine activation leads to acidification and increases maturation of *Mycobacterium avium*-containing phagosomes in murine macrophages. J. Immunol. **160:**1290–1296.

54. **Snyderman, R., H. Shin, and A. M. Dannenberg, Jr.** 1972. Macrophage proteinase and inflammation: the production of chemotactic activity from the fifth complement by macrophage proteinase. J. Immunol. **109:**896–898.

55. **Sturgill-Koszycki, S., and M. S. Swanson.** 2000. *Legionella pneumophila* replication vacuoles mature into acidic, endocytic organelles. J. Exp. Med. **192:**1261–1272.

56. **Suga, M., A. M. Dannenberg, Jr., and S. Higuchi.** 1980. Macrophage functional heterogeneity in vivo. Macrolocal and microlocal macrophage activation, identified by double-staining tissue sections of BCG granulomas for pairs of enzymes. Am. J. Pathol. **99:**305–323.

57. **Talaat, A. M., R. Reimschuessel, S. S. Wasserman, and M. Trucksis.** 1998. Goldfish, *Carassius auratus*, a novel animal model for the study of *Mycobacterium marinum* pathogenesis. Infect. Immun. **66:**2938–2942.

58. **Travis, W. D., L. B. Travis, G. D. Roberts, D. W. Su, and L. W. Weiland.** 1985. The histopathologic spectrum in *Mycobacterium marinum* infection. Arch. Pathol. Lab. Med. **109:**1109–1113.

59. **Via, L. E., R. A. Fratti, M. McFalone, E. Pagan-Ramos, D. Deretic, and V. Deretic.** 1998. Effects of cytokines on mycobacterial phagosome maturation. J. Cell Sci. **111:**897–905.

60. **Xu, S., A. Cooper, S. Sturgill-Koszycki, T. van Heyningen, D. Chatterjee, I. Orme, P. Allen, and D. G. Russell.** 1994. Intracellular trafficking in *Mycobacterium tuberculosis* and *Mycobacterium avium*-infected macrophages. J. Immunol. **153:**2568–2578.

61. **Zychlinsky, A., and P. J. Sansonetti.** 1997. Apoptosis as a proinflammatory event: what can we learn from bacteria-induced cell death? Trends Microbiol. **5:**201–204.